Cooling Enhancements in Thin Films Supported by Flexible Complex Seals in the Presence of Ultrafine Suspensions

A.-R. A. Khaled
Department of Mechanical Engineering,
The Ohio State University,
Columbus, OH 43210

K. Vafai
Department of Mechanical Engineering,
University of California, Riverside,
Riverside, CA 92521

Flow and heat transfer inside thin films supported by flexible soft seals having voids of a stagnant fluid possessing a large coefficient of volumetric thermal expansion β_T are studied in the presence of suspended ultrafine particles. The study is conducted under periodically varying thermal load conditions. The governing continuity, momentum and energy equations are non-dimensionalized and reduced to simpler forms. The deformation of the seal is related to the internal pressure and lower plate's temperature based on the theory of linear elasticity and a linearized model for thermal expansion. It is found that enhancements in the cooling are achieved by an increase in the volumetric thermal expansion coefficient, thermal load, thermal dispersion effects, softness of the supporting seals and the thermal capacitance of the coolant fluid. Further, thermal dispersion effects are found to increase the stability of the thin film. The noise in the thermal load is found to affect the amplitude of the thin film thickness, Nusselt number and the lower plate temperature however it has a negligible effect on their mean values.
[DOI: 10.1115/1.1597612]

Keywords: Cooling, Enhancement, Film, Heat Transfer, Seals

1 Introduction

Thin films are widely used in cooling of many heating sources such as electronic components. These elements use thin films in their cooling systems as in flat heat pipes (Moon et al. [1]) or microchannel heat sinks (Fedorov and Viskanta [2], Zhu and Vafai [3]). Many ideas are proposed to enhance the cooling load of thin films. For example, Bowers and Mudawar [4] showed that two phase flow in minichannel is capable of removing maximum heat fluxes generated by electronic packages yet the system may become unstable near certain operating conditions. Further, the use of porous medium in cooling of electronic devices (Hadim [5]) was found to enhance heat transfer due to increases in the effective surface area. However, the porous medium creates a substantial increase in the pressure drop inside the thin film.

Khaled and Vafai [6] showed that cooling effects achieved by having thin films supported by soft seals are more than when these seals are stiff. This is due to an increase in the thickness resulting from pressure forces when soft seals are used. Additional cooling can be achieved if the thin film thickness is allowed to increase by an increase in the thermal load which will cause the coolant flow rate to increase. This task can be reached if the sealing assembly supporting the plates of the thin film is composed of the following: soft seals and voids of a stagnant fluid having a large value of the volumetric thermal expansion coefficient β_T. This proposed sealing assembly will be named a ''flexible complex seal'' and will be used regularly in the text. It is worth noting that the enhancement in the cooling when flexible complex seals are used is expected to be apparent at larger thermal loads for stagnant liquids while it is prominent at lower temperatures for stagnant gases, especially ideal gases. This is because the volumetric thermal expansion coefficient increases for liquids and decreases for gases as their temperatures increases.

In the presence of periodic external thermal loads, the thickness of a thin film supported by a flexible seal containing voids of a fluid having a large β_T value is expected to be periodic. This is because the stagnant fluid expands during maximum thermal load intervals allowing for a relaxation in the thin film thickness which causes a flooding of the coolant. On the other hand, the thin film is squeezed during minimum thermal load intervals due to the contraction in the stagnant fluid in the sealing assembly voids. Several authors have considered flow inside squeezed thin films like Langlois [7] who performed an analytical study for flow inside isothermal oscillatory squeezed films having the fluid density varying with pressure. However, only few of them have analyzed heat transfer inside squeezed thin films such as Hamza [8], Bhattacharyya et al. [9] and Debbaut [10]. In these works, the squeezing was not of an oscillatory type. All of these works considered a predetermined squeezing effect at the plates of the thin film. Recently, Khaled and Vafai [11] considered flow and heat transfer inside incompressible oscillatory squeezed thin films.

One of the advantages of using flexible complex seals is that the increase in the coolant flow rate because of thermal expansion effects produces an additional cooling in the presence of suspended ultrafine particles (Li and Xuan [12]). This is because the chaotic movement of the ultrafine particles, the thermal dispersion, increases with the flow where it is modeled in the energy equation by introducing an effective thermal conductivity of the coolant (Xuan and Roetzel [13]). Further, large fluctuation rates that can be generated in the flow during severe squeezing conditions tend to increase the chaotic motions of the particles in the fluid which increases the energy transport in the coolant.

In this work, the enhancement in the cooling process inside thin films supported by flexible complex seals in the presence of suspended ultrafine particles is investigated. The lower plate of the examined thin film is considered to be under a periodically varying heat flux. The thin film thickness is related to the thermal load and the internal pressure through the volumetric thermal expansion coefficient of the stagnant fluid and the theory of linear elasticity applied to the supporting seals. The governing equations for flow and heat transfer are properly non-dimensionalized and reduced into simpler equations for low Reynolds numbers. The re-

Contributed by the Heat Transfer Division for publication in the JOURNAL OF HEAT TRANSFER. Manuscript received by the Heat Transfer Division November 26, 2002; revision received May 9, 2003. Associate Editor: H. Bau.

sulting equations are then solved numerically to determine the effects of the thermal load, volumetric thermal expansion coefficient of the stagnant fluid, the softness of the seal, thermal capacitance of the working fluid and the squeezing number on the dynamics and thermal characteristic of the thin films supported by flexible complex thin films.

2 Problem Formulation

Figure 1 shows a thin film having a flexible complex seal. It is composed of the coolant flow, the working fluid, passage and the sealing assembly. This assembly contains closed voids filled with a stagnant fluid having relatively a large coefficient of volumetric thermal expansion. The sealing assembly contains also soft seals in order to allow the thin film to expand. A candidate for the soft seal is the closed cell rubber foam [14]. Any excessive heat increases the temperature of the hot plate thus the stagnant fluid becomes warmer and expands. The seals are soft enough so that the expansion results in an increase in the separation between the lower and the upper plates. Accordingly, the flow resistance of the working fluid passage decreases causing a flooding of the coolant. As a result, the excessive heating from the source is removed. It is worth noting that the soft seals can be placed between special guiders as shown in Fig. 1(*b*). As such, side expansion of the seals can be minimized and the transverse thin film thickness expansion is maximized.

The analysis is concerned with a thin film that has a small thickness h compared to its length B and its width D. Therefore, a two-dimensional flow is assumed. The x-axis is taken along the axial direction of the thin film while y-axis is taken along its thickness as shown in Fig. 1(*a*). Further, it is assumed in this work that the film thickness is independent of the axial coordinate. For example, this occurs in two main cases: symmetric thin films hav-

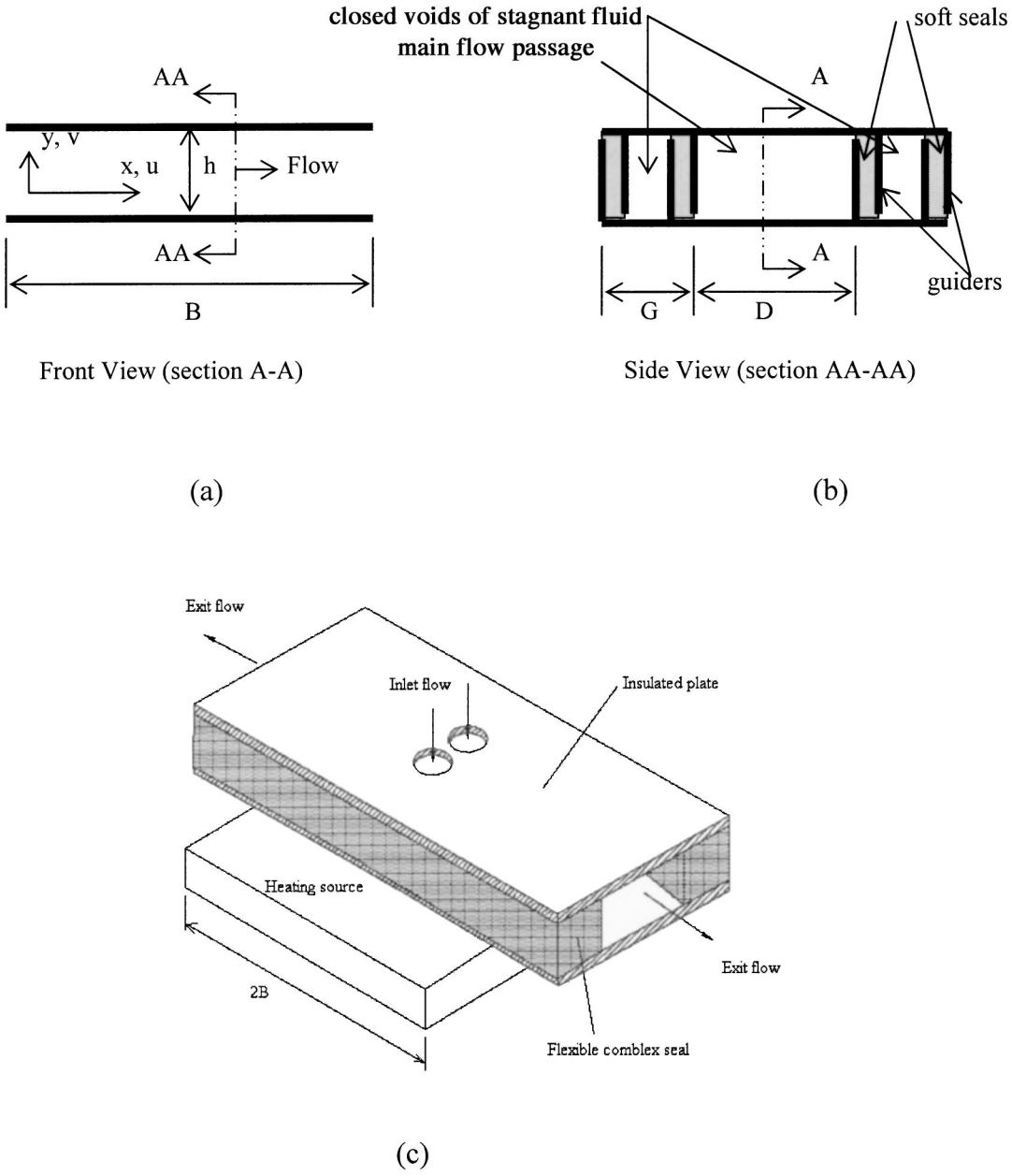

Fig. 1 Schematic diagram for a thin film with flexible complex seal and the corresponding coordinate system: (*a*) front view, (*b*) side view, and (*c*) a three dimensional diagram

ing a fluid injected from the center as shown in Fig. 1(*c*) and in multiple passages thin films having alternating coolant flow directions.

The lower plate of the thin film is assumed to be fixed to a heating source while the upper plate is attached to the lower plate by flexible complex seals allowing it to expand. The motion of the upper plate due to both internal variations in the stagnant fluid temperature and the induced internal pressure pulsations as a result of oscillating thermal loads is expressed according to the following relation:

$$H \equiv \frac{h}{h_o} = (1 + H_T + H_p) \tag{1}$$

where h, h_o, and H are the thin film thickness, a reference film thickness and the dimensionless thin film thickness, respectively. The variables H_T and H_p are the dimensionless motion of the upper plate due to the thermal expansion of the stagnant fluid and the dimensionless motion of the upper plate as a result of the deformation of seals due to the average internal pressure of the working fluid, respectively. It is assumed that the fluid is Newtonian having constant average properties except for the thermal conductivity.

The general two-dimensional continuity, momentum and energy equations for a laminar flow of the working fluid inside the thin film are given as

$$\frac{\partial u}{\partial x} + \frac{\partial v}{\partial y} = 0 \tag{2}$$

$$\rho\left(\frac{\partial u}{\partial t} + u\frac{\partial u}{\partial x} + v\frac{\partial u}{\partial y}\right) = -\frac{\partial p}{\partial x} + \mu\left(\frac{\partial^2 u}{\partial x^2} + \frac{\partial^2 u}{\partial y^2}\right) \tag{3}$$

$$\rho\left(\frac{\partial v}{\partial t} + u\frac{\partial v}{\partial x} + v\frac{\partial v}{\partial y}\right) = -\frac{\partial p}{\partial y} + \mu\left(\frac{\partial^2 v}{\partial x^2} + \frac{\partial^2 v}{\partial y^2}\right) \tag{4}$$

$$\rho c_p\left(\frac{\partial T}{\partial t} + u\frac{\partial T}{\partial x} + v\frac{\partial T}{\partial y}\right) = \frac{\partial}{\partial x}\left(k\frac{\partial T}{\partial x}\right) + \frac{\partial}{\partial y}\left(k\frac{\partial T}{\partial y}\right) \tag{5}$$

where T, u, v, ρ, p, μ, c_p, and k are temperature, dimensional axial velocity, dimensional normal velocity, average density, pressure, average dynamic viscosity, average specific heat and the thermal conductivity, respectively. The previous fluid properties are for the pure working fluid in the case where the fluid is free from any suspensions. In the presence of suspended ultrafine particles, the previous properties will be for an approximated new continuum fluid composed from the mixture of the pure fluid and the suspensions (Xuan and Roetzel [13]). The new properties are related to the fluid and the particle properties through the volume fraction of the suspended particles inside the thin film and the thermal dispersion parameter. These relations are found in the literature (e.g., Xuan and Roetzel [13]).

The following dimensionless variables will be utilized to nondimensionalize Eqs. (2)–(5):

$$X = \frac{x}{B} \quad Y = \frac{y}{h_o} \tag{6a,b}$$

$$\tau = \omega t \tag{6c}$$

$$U = \frac{u}{(\omega B + V_o)} \quad V = \frac{v}{h_o \omega} \tag{6d,e}$$

$$\Pi = \frac{p - p_e}{\mu\left(\omega + \frac{V_o}{B}\right)\varepsilon^{-2}} \tag{6f}$$

$$\theta = \frac{T - T_1}{(q_o h_o)/k_o} \tag{6g}$$

where ω, T_1, p_e, q_o, and V_o are the reference frequency of thermal load, inlet temperature of the fluid, a constant representing the exit pressure, reference heat flux and a constant representing a reference dimensional velocity, respectively. The term k_o corresponds to the working fluid thermal conductivity in the absence of any suspensions while it is the stagnant thermal conductivity, free from the dispersion term, for the dilute mixture between the fluid and the ultrafine suspensions. The stagnant thermal conductivity has usually an enhanced value when compared to that of the pure fluid for metallic particles (Eastman et al. [15]).

It is assumed that the upper plate is insulated to simplify the analysis and that the lower plate is subjected to a periodically varying wall heat flux q_L condition according to the following relation:

$$q_L = q_o(1 + \beta_q \sin(\gamma\omega t)) \tag{7}$$

where β_q and γ are the dimensionless amplitude of the lower plate's heat flux and a dimensionless frequency, respectively. The variables X, Y, τ, U, V, Π, and θ are the dimensionless forms of x, y, t, u, v, p, and T variables, respectively. The parameter ε appearing in Equation (6*f*) is the perturbation parameter, $\varepsilon = h_o/B$.

For the thin film shown in Fig. 1(*c*), the displacement of the upper plate due to internal pressure variations is related to the average dimensionless pressure of the working fluid, Π_{AVG}, through the theory of linear elasticity by the following relation:

$$H_p = F_n \Pi_{\mathrm{AVG}} \tag{8}$$

This is based on the fact that the upper plate is assumed to be rigid and that the applied force on an elastic material (the soft seal is assumed to behave as an elastic material) is proportional to the elongation of this material (Norton [16]). The parameter F_n is referred to as the fixation parameter and it is a measure of the softness of the seal, soft seals have large F_n values. It is equal to

$$F_n = \frac{\mu(V_o + \omega B)}{E\varepsilon^2 d_s}, \tag{9}$$

where E and d_s are the effective modulus of elasticity for the complex seal and a characteristic parameter which depends on the seal's dimensions and the thin film width D, respectively. The quantity d_s is equal to the effective dimension of the seal's cross section times the ratio of the total length of the seal divided by the thin film width D. The seal is considered to have isotropic properties. Further, the effective dimension of the seals times their total length represents the contact area between the seals and the upper or lower plates when the seals have a rectangular cross section as shown in Fig. 1. Other than this, the effective diameter requires a theoretical determination.

In this work, the analysis is performed for relatively small thermal load frequencies in order to ascertain that squeezing generated flows have relatively small Reynolds numbers. For these frequencies, Eq. (8) is applicable and the inertia effect of the upper plate is negligible. Moreover, the increase in the thickness due to a pressure increase in the thin film causes a reduction in the stagnant fluid pressure. This action stiffens the sealing assembly. Therefore, the parameter E is considered to be the effective modulus of elasticity for the sealing assembly not for the seal itself. Practically, the void width G is assumed to be large enough such that a small increase in the stagnant fluid pressure due to the expansion can support the associated increase in the elastic force on the seal.

The dimensionless displacement of the upper plate due to thermal expansion is related to the dimensionless average temperature of the lower plate, $(\theta_W)_{\mathrm{AVG}}$, by the following linearized model:

$$H_T = F_T(\theta_W)_{\mathrm{AVG}} \tag{10}$$

where F_T is named the dimensionless thermal expansion parameter. It is equal to

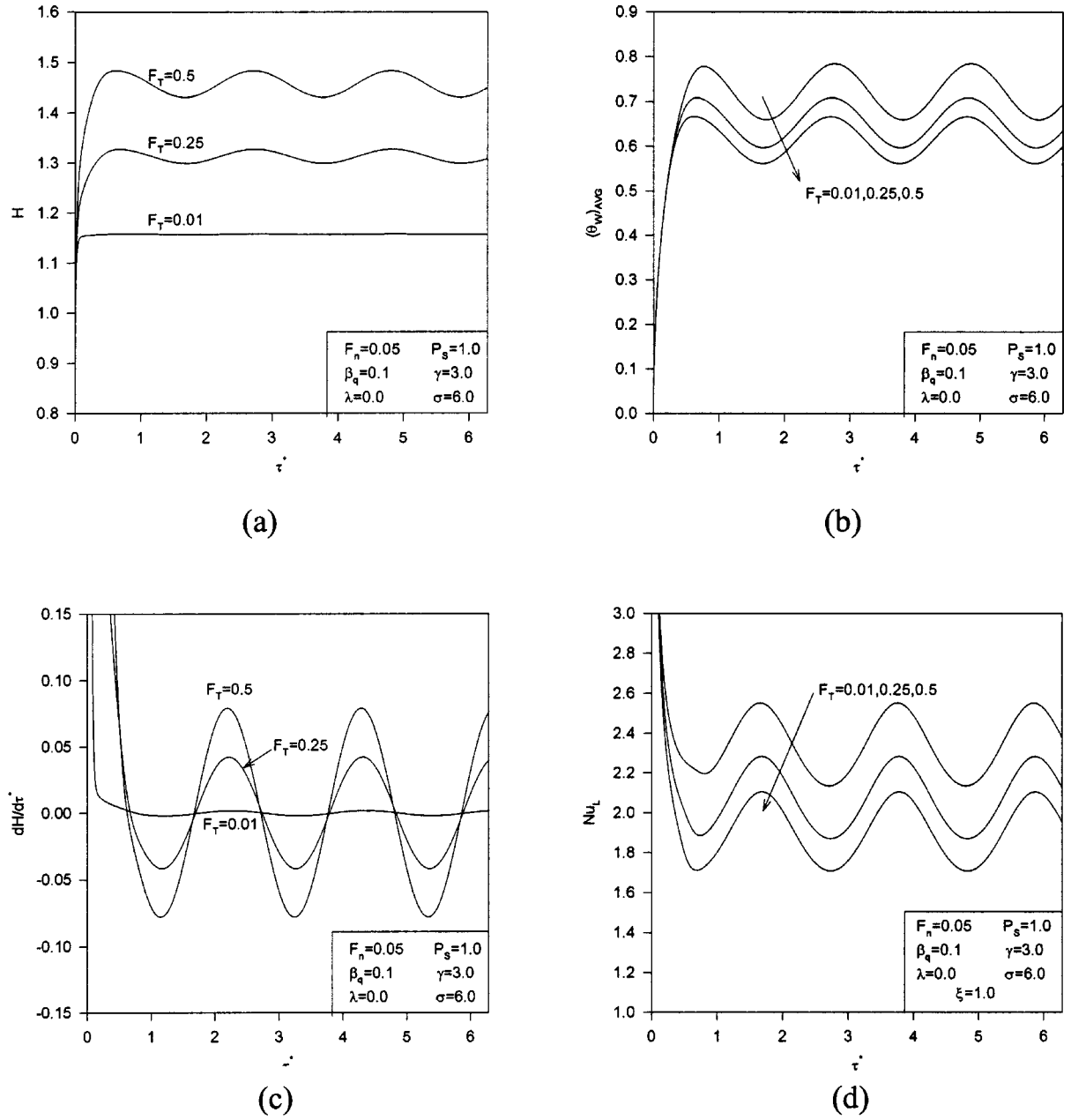

Fig. 2 Effects of the dimensionless thermal expansion parameter F_T on (*a*) dimensionless thin film thickness H, (*b*) dimensionless average lower plate temperature $(\theta_W)_{AVG}$, (*c*) $dH/d\tau$, and (*d*) exit Nusselt number Nu_L

$$F_T = A^* \frac{\beta_T q_o h_o}{k_o} C_F \tag{11}$$

where A^* is a constant depending on the voids dimensions and geometry. The parameter β_T is the volumetric thermal expansion coefficient of the stagnant fluid in its approximate form:

$$\beta_T \approx (1/V_{so})[(V_s - V_{s1})/(T_s - T_1)]|_{p_{s1}}$$

evaluated at the pressure p_{s1} corresponding to the stagnant fluid pressure at the inlet temperature T_1. The quantities V_{s1} and V_s represent the void volumes at normal operating conditions when the stagnant fluid is at T_1 and at the present stagnant fluid temperature T_s, respectively. The parameter V_{so} represents the void volume at the reference condition. The factor C_F represents the volumetric thermal expansion correction factor. This factor is introduced in order to account for the increase in the stagnant pressure due to the increase in the elastic force in the seal during the expansion which tends to decrease the effec-tive volumetric thermal expansion coefficient. It approaches one as the void width G increases and it needs to be determined theoretically.

The parameter F_T is enhanced at elevated temperatures for liquids and at lower temperature for gases because β_T increases for liquids and decreases for gases as the stagnant temperature increases. Dimensionless thermal expansion parameter is also enhanced by a decrease in k_o, an increase in q_o, an increase in F_n or by increases in h_o. It is worth noting that Eq. (10) is based on the assumption that the stagnant fluid temperature is similar to the lower plate temperature since entire void surfaces are considered insulated except that facing the lower plate. Furthermore, the heat flux of the heating source is applied on the portion of the lower plate that is facing the working fluid. The other portion which faces the seals is taken to be isolated from the heating source and

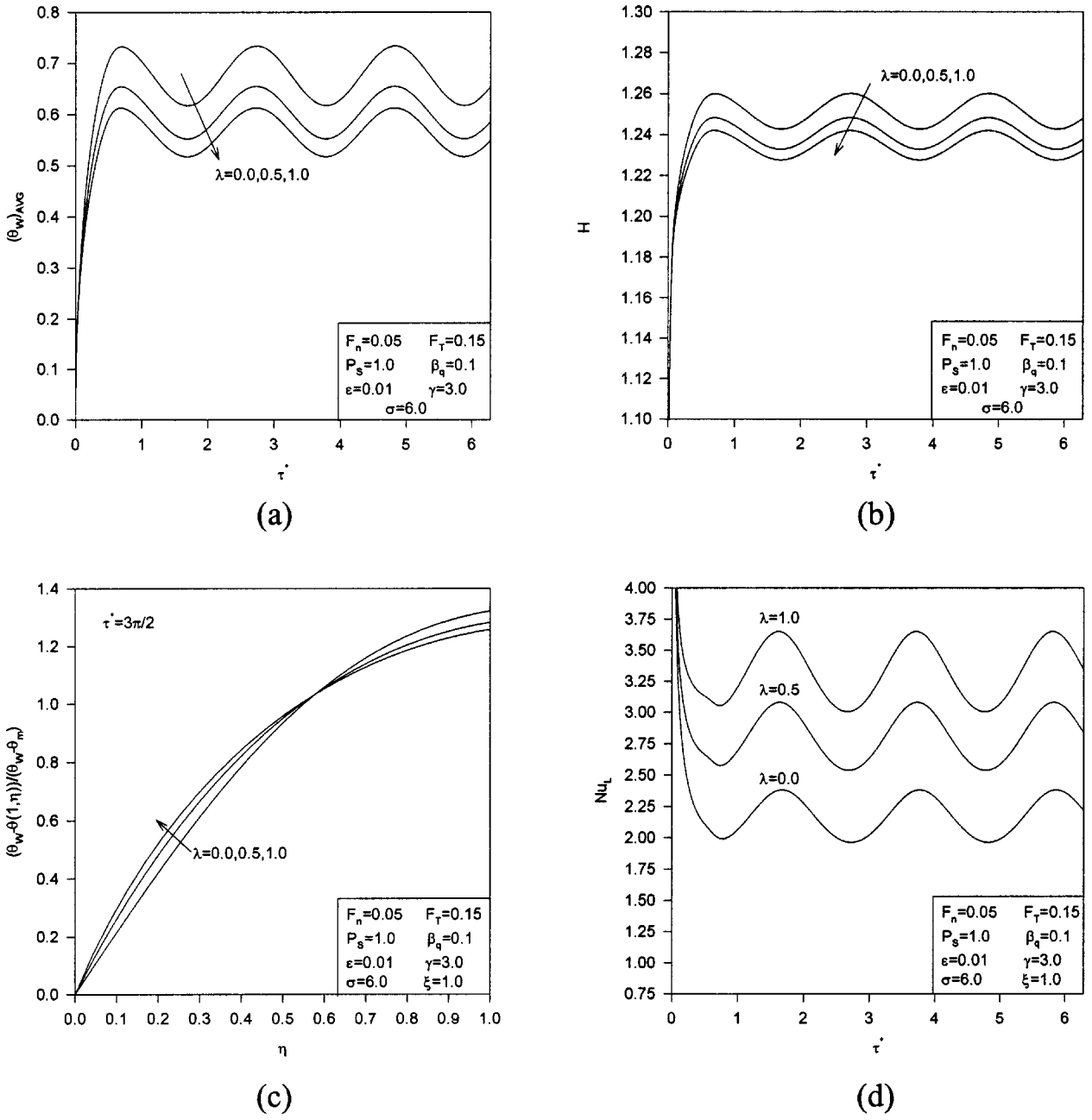

Fig. 3 Effects of the dimensionless thermal dispersion parameter λ on (*a*) dimensionless average lower plate temperature $(\theta_W)_{AVG}$, (*b*) dimensionless thickness *H*, (*c*) temperature Profile, and (*d*) exit Nusselt number Nu_L

the environment to minimize the variation in the lower plate temperature along the width direction.

In the presence of suspended ultrafine particles in the working fluid, the thermal conductivity of the working fluid composed from the pure fluid and suspensions is expected to vary due to the thermal dispersion (Xuan and Roetzel [13]). To account for these variations, the following model which is similar to Xuan and Roetzel [13] model that linearly relates the effective thermal conductivity of the working fluid to the fluid speed is utilized:

$$k(X,Y,\tau)=k_o(1+\lambda\sqrt{U^2(X,Y,\tau)+\Lambda^2V^2(X,Y,\tau)})=k_o\phi(X,Y,\tau) \tag{12}$$

where λ and Λ are the dimensionless thermal dispersion coefficient and the reference squeezing to lateral velocity ratio. They are

$$\lambda=C^*(\rho c_p)h_o(V_o+\omega B) \tag{13a}$$

$$\Lambda=\frac{\varepsilon\sigma}{12} \tag{13b}$$

where C^* is the coefficient of the thermal dispersion which depends on the diameter of the ultrafine particles, its volume fraction (ratio of the particles volume to the total thin film volume), and both fluid and ultrafine particles properties.

It is worth noting that the term ultrafine suspensions indicate that the particle is extremely small compared with the thickness of the thin film. The coefficient C^* is expected to increase by an increase in the diameter of the particles, their volume fraction, their surface roughness and the working fluid Prandtl number, $\mathrm{Pr}=(\rho c_p \upsilon)/k_o$. On the other hand, the stagnant thermal conductivity k_o increases with an increase in both the volume fraction and the surface area of the particles (Xuan and Roetzel [13]). In the

work of Li and Xuan [12], they showed experimentally that dilute mixture of ultrafine suspensions and water produced no significant change in the pressure drop compared to pure water which reveals that the viscosity is a weak function of the fluid dispersion for a dilute mixture.

Generally, flows inside thin films are in laminar regime and could be creep flows as in lubrication. Therefore, the low Reynolds numbers (the modified lateral Reynolds number $\mathrm{Re}_L=(V_o h_o)\varepsilon/\upsilon$ and the squeezing Reynolds number $\mathrm{Re}_S=(h_o^2\omega)/\upsilon$) flow model is adopted here. This model neglects the transient and convective terms in momentum equations, Eqs. (3) and (4). These terms become incomparable to the pressure gradient and diffusive terms for small squeezing frequencies and reference velocities. The application of this model to Eqs. (2)–(4) and the outcome of the dimensionalization of the energy equation, Eq. (5), result in the following reduced non-dimensionalized equations:

$$U=\frac{1}{2}\frac{\partial\Pi}{\partial X}H^2\left(\frac{Y}{H}\right)\left(\frac{Y}{H}-1\right) \tag{14}$$

$$V=\frac{dH}{d\tau}\left(3\left(\frac{Y}{H}\right)^2-2\left(\frac{Y}{H}\right)^3\right) \tag{15}$$

$$\frac{\partial}{\partial X}\left(H^3\frac{\partial\Pi}{\partial X}\right)=\sigma\frac{\partial H}{\partial\tau} \tag{16}$$

$$P_S\left(\frac{\partial\theta}{\partial\tau}+\frac{12}{\sigma}U\frac{\partial\theta}{\partial X}+V\frac{\partial\theta}{\partial Y}\right)=\frac{\partial}{\partial Y}\left(\phi\frac{\partial\theta}{\partial Y}\right) \tag{17}$$

Note that Eq. (17) is based on the assumption that the axial conduction is negligible when compared to the transverse conduction. The parameters σ and P_S are referred to as the squeezing number and the thermal squeezing parameter, respectively. They are defined as

$$\sigma=\frac{12}{1+\dfrac{V_o}{\omega B}}\qquad P_S=\frac{\rho c_p h_o^2\omega}{k_o} \tag{18}$$

Both inlet and exit dimensionless pressures are assumed constant and the following relationship is obtained between the inlet dimensionless pressure and the squeezing number based on the assumption that the reference velocity V_o represents the average velocity in the thin film at zero values of F_T and F_n:

$$\Pi_i=12-\sigma \tag{19}$$

Accordingly, the dimensionless pressure gradient, the dimensionless pressure and the average dimensionless pressure Π_{AVG} inside the thin film are related to the squeezing number through the following equations:

$$\frac{\partial\Pi(X,\tau)}{\partial X}=\frac{\sigma}{H^3}\frac{dH}{d\tau}\left(X-\frac{1}{2}\right)-(12-\sigma) \tag{20}$$

$$\Pi(X,\tau)=\frac{\sigma}{2H^3}\frac{dH}{d\tau}(X^2-X)-(12-\sigma)(X-1) \tag{21}$$

$$\Pi_{\mathrm{AVG}}(\tau)=-\frac{\sigma}{12H^3}\frac{dH}{d\tau}+\frac{(12-\sigma)}{2} \tag{22}$$

Thermal Boundary Conditions. The dimensionless thermal boundary conditions for the previously defined problem are taken as follows:

$$\theta(X,Y,0)=0,\quad \theta(0,Y,\tau)=0,$$

$$\frac{\partial\theta(X,0,\tau)}{\partial Y}=-(1+\beta_q\sin(\gamma\tau)),\quad \frac{\partial\theta(X,H,\tau)}{\partial Y}=0 \tag{23}$$

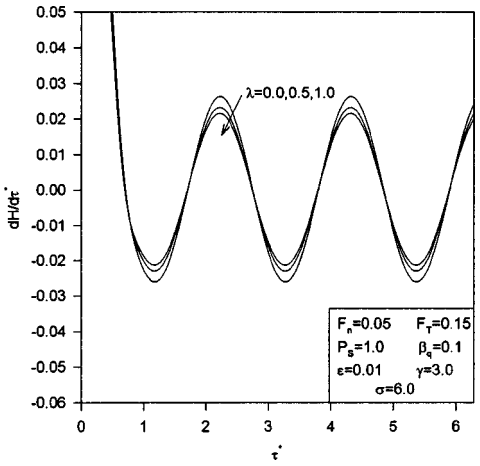

Fig. 4 Effects of the dimensionless dispersion parameter λ on the time variation of the dimensionless thin film thickness $dH/d\tau$

Based on the physical conditions, the Nusselt number is defined as

$$\mathrm{Nu}_L(X,\tau)\equiv\frac{h_c h_o}{k}=\frac{1}{\theta(X,0,\tau)-\theta_m(X,\tau)}=\frac{1}{\theta_W(X,\tau)-\theta_m(X,\tau)} \tag{24}$$

The parameter θ_m is the dimensionless mean bulk temperature. It is given as

$$\theta_m(X,\tau)=\frac{1}{U_m(X,\tau)H}\int_0^H U(X,Y,\tau)\,\theta(X,Y,\tau)\,dY$$
$$U_m(X,\tau)=\frac{1}{H}\int_0^H U(X,Y,\tau)\,dY \tag{25}$$

where U_m is the dimensionless average velocity at a given section.

3 Numerical Procedure

The procedure for the numerical solution is summarized as follows:

1) Initially, a value for H_T is assumed.

2) At the present time, the dimensionless thickness of the thin film H is determined by solving Eqs. (1), (8), (9), and (22), simultaneously, using an explicit formulation. The velocity field, U and V, is then determined from Eqs. (14), (15), and (20).

3) At the present time, the reduced energy equation Eq. (17) is transferred into one with constant boundaries using the following transformations: $\tau^*=\tau$, $\xi=X$ and $\eta=Y/H$. A tri-diagonal solution (Blottner [17]) was implemented along with a marching scheme. Backward differencing was chosen for the axial convective and transient terms and central differencing was selected for the derivatives with respect to η. The values of 0.008, 0.03, 0.001 were chosen for $\Delta\xi$, $\Delta\eta$, and $\Delta\tau^*$, respectively.

4) H_T is updated from Eq. (10) and steps (2)–(4) are repeated until

$$\left|\frac{(H_T)_{\mathrm{new}}-(H_T)_{\mathrm{old}}}{(H_T)_{\mathrm{new}}}\right|<10^{-6} \tag{26}$$

5) The converged solution for the flow and heat transfer inside the thin film is determined at the present time.

6) Time is advanced by $\Delta\tau^*$ and steps (1)–(5) are repeated.

Numerical investigations were performed using different mesh sizes and time steps to assess and ascertain grid and time step independent results. It was found that any reduction in the values of $\Delta\xi$, $\Delta\eta$ and $\Delta\tau^*$ below $\Delta\xi=0.008$, $\Delta\eta=0.03$, and $\Delta\tau^*=0.001$ results in less than 0.2% error in the results.

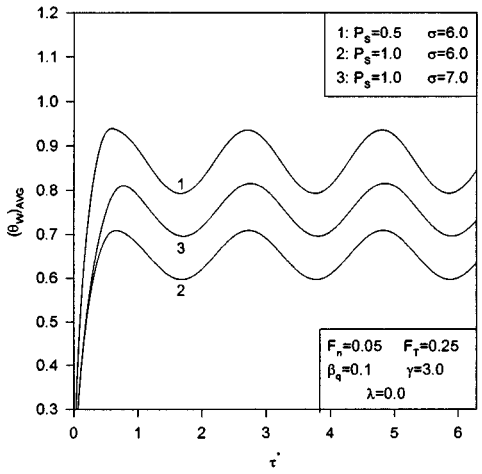

(a)

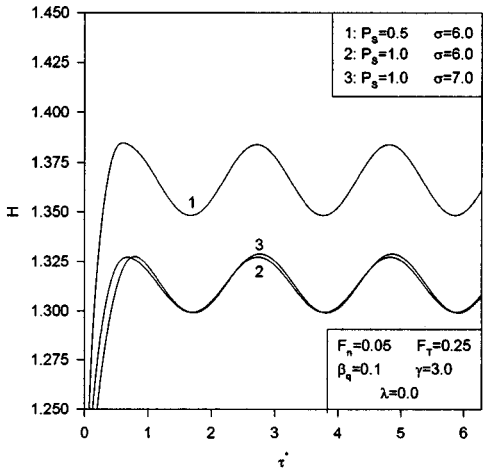

(b)

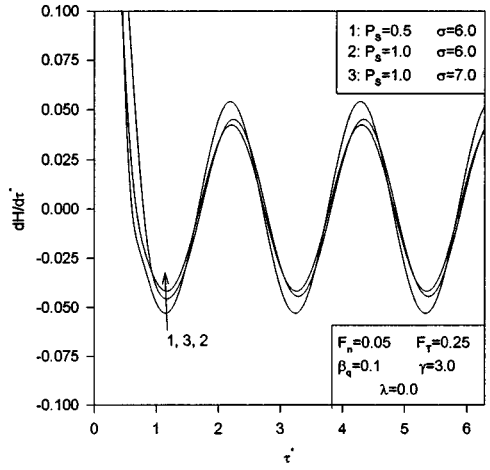

(c)

Fig. 5 Effects of the thermal squeezing parameter P_S and the squeezing number σ on (a) dimensionless average lower plate temperature $(\theta_W)_{AVG}$, (b) dimensionless thin film thickness H, and (c) $dH/d\tau$

In the results, the maximum value of the parameters P_S is chosen to be 1.0. Beyond this value, the error associated with the low Reynolds number model will increase for moderate values of the dimensionless thermal expansion parameter, fixation parameter, and the Prandtl number. As an example, the order of transient and convective terms in the momentum equations were found to be less 1.0% that of the diffusive terms for $P_S=1.0$, Pr=6.0, $F_n=0.05$, $F_T=0.25$, $\beta_q=0.1$, and $\sigma=6.0$. The parameters correspond, for example, to a thin film filled with water and having $B=D=60$ mm, $h_o=0.3$ mm, $d_s=0.5$ mm, $\omega=2.0$ s^{-1}, $V_o=0.12$ m/s, and $E=1.6(10^5)$ pa.

4 Results and Discussions

Ideal gases produce a 15% increase in the void volume at room conditions for a 45°C maximum temperature difference. Further, Li and Xuan [12] reported a 60% increase in the convective heat transfer coefficient for a volume fraction of copper ultrafine particles of 2.0%. Accordingly, the parameters F_T and λ were varied until comparable changes have been attained in the dimensionless thin film thickness and the Nusselt number.

4.1 Effects of Dimensionless Thermal Expansion Parameter. Figure 2(*a*) illustrates the effects of the dimensionless thermal expansion parameter F_T on the dimensionless thickness H of the thin film. The parameter F_T can be increased either by an increase in the volumetric thermal expansion coefficient of the stagnant fluid or by an increase in dimensional reference temperature $(q_o h_o)/k_o$. Both factors make the flexible complex seal softer thus dimensionless thickness H is increased as F_T increases as shown in Fig. 2(*a*). This allows more coolant to flow causing reductions in the average dimensionless lower plate's temperature

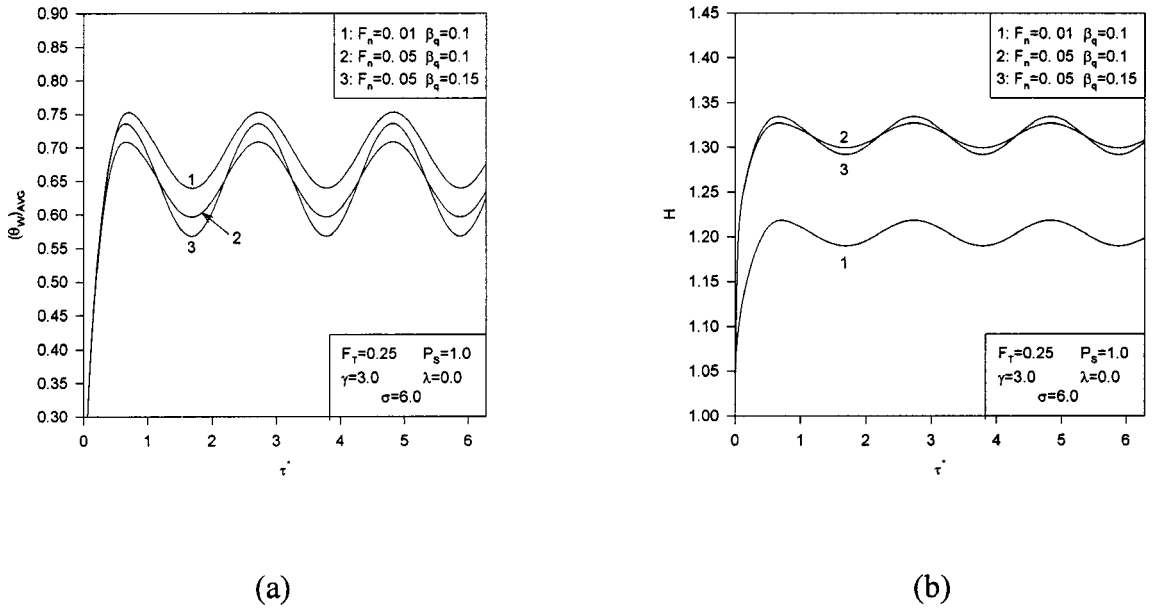

Fig. 6 Effects of the fixation parameter F_n and the dimensionless thermal load amplitude β_q on (a) dimensionless average lower plate temperature $(\theta_W)_{AVG}$, and (b) dimensionless thin film thickness H

$(\theta_W)_{AVG}$ as clearly seen in Fig. 2(*b*) which can provide additional cooling to any heated surface such as surfaces of electronic components.

Figure 2(*b*) can be also read as follows: as thermal load increases, the average lower plate's temperature increases however this increase can be reduced by using a flexible complex seal. This additional cooling is obtained with no need for external controlling devices which provides extra safety for an electronic component, as an example for a heated surface, when their thermal loads increase over the projected capacity. The fluctuation rate at the upper plate, $|dH/d\tau|$, is noticed to increase as F_T increases as shown in Fig. 2(*c*). This could be an advantage for the cooling process especially at high levels of fluctuation rates since it will enhance the thermal dispersion in the coolant when suspended ultrafine particles are present. The Nusselt number is decreased as F_T increases as shown in Fig. 2(*d*) because it is inversely proportional to H. This is the reason for the fact that the percentage decrease in lower plate temperatures is lower than the percentage increase in the thin film thickness as F_T increases.

4.2 Effects of Dimensionless Thermal Dispersion Parameter. Figure 3(*a*) describes the effects of the dimensionless thermal dispersion parameter λ of the coolant fluid on the average lower plate's temperature of the thin film. This parameter can be increased either by increasing the diameter of the ultrafine particles or increasing the roughness of these particles while keeping a fixed volume fraction inside the coolant. This insures that thermal squeezing parameter remains constant. Figure 3(*a*) physically shows that the thermal dispersion can provide additional cooling to a heated element, thus it causes an additional reduction in the average dimensionless lower plate temperature $(\theta_W)_{AVG}$. Part of this cooling is due to the expansion process since it results in flooding of the working fluid which increases the irregularity and the random motion of the particles. This causes additional enhancements in the energy exchange rate. Another Part for the enhancement in the cooling is attributed to the fact that the noise in the thermal load, especially those having heterogeneous fluctuation rates, produces additional squeezing due to the velocities that appear in Eq. (12).

Due to the reduction in the lower plates temperatures as λ increases, the dimensionless thin film thickness decreases as λ increases as depicted in Fig. 3(*b*). It is worth noting that additional enhancements in the thermal dispersion effect are expected as both the perturbation parameter and the squeezing number increase as suggested by Eqs. (12) and (13). Both effects result in a magnification in the fluctuation rates in the flow which causes additional increases in the cooling process. In our example, the perturbation parameter and the fluctuation rates are small and their effects are not noticeable.

The reduction in thermal resistance across the transverse direction when λ increases causes the temperature profiles to be more flattened as λ increases as seen in Fig. 3(*c*). Accordingly, the Nusselt number increases as λ increases as seen in Fig. 3(*d*). It can be seen in Fig. 4 that the fluctuation rate at the upper plate, $|dH/d\tau|$, decreases as λ increases. As a result, ultrafine particle suspensions inside thin films supported by flexible complex seals not only cause enhancements in heat transfer but also make these thin films dynamically more stable. In this example, an increase in λ between zero and unity cause a reduction in the average lower temperature by dimensionless temperature of 0.12 and an increase in the Nusselt number by 50%.

4.3 Effects of Thermal Squeezing Parameter and the Squeezing Number. Figure 5(*a*) shows the effects of the thermal squeezing parameter P_S and the squeezing number σ on the average dimensionless lower plate temperature $(\theta_W)_{AVG}$. It is clearly seen that the lower plate temperature decreases as P_S increases and as σ decreases. Both effects tend to increase thermal convection which decreases the lower plate temperature. The increase in P_S means an increase in the thermal capacitance of the working fluid and a decrease in σ indicates an increase in the reference velocity. Accordingly, the dimensionless thickness H decreases as P_S increases as shown in Fig. 5(*b*). In addition, the pressure force inside the thin film increases as σ decreases causing an increase in H_p while H_T decreases as σ decreases due to the enhancement in the cooling. As a result, the thin film thickness is noticed to vary slightly when σ decreases as illustrated in Fig. 5(*b*). As seen in Fig. 5(*c*), the fluctuation rate at the upper plate is found to increase as σ increases while it decreases as P_S increases. Also, the fluctuation rate at the upper plate is shown to more pronounced to P_S more than to σ.

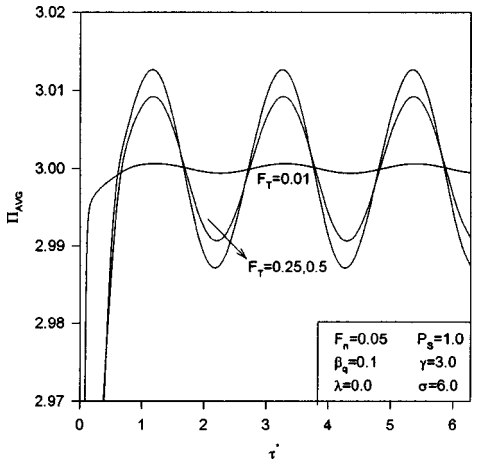

Fig. 7 Effects of the dimensionless thermal expansion parameter F_T on the average dimensionless pressure inside the thin film Π_{AVG}

4.4 Effects of the Fixation Parameter and the Amplitude of the Thermal Load. Figure 6(*a*) shows the effects of the fixation parameter F_n and the dimensionless amplitude of the thermal load β_q on the average dimensionless lower plate temperature $(\theta_W)_{\mathrm{AVG}}$. Since soft seals possess large F_n values, H increases and lower plate temperature decreases as F_n increases as shown in Figs. 6(*a*) and 6(*b*). Further, these figures show that an increase in the amplitude of the heat flux results in an increase in the fluctuation rate at the upper plate and the lower plate temperature but their mean values are almost unaffected.

4.5 Effects of Dimensionless Thermal Expansion Parameter on Average Pressure. Figure 7 shows the effects of F_T on the average dimensionless pressure inside a thin film supported by a flexible complex seal. The periodic behavior of the heat flux results in a periodic variation in the average pressure inside the thin film. The fluctuation in the pressure increases as F_T increases as seen in Fig. 7. Further, it is noticed that the thermal load exceeding the internal pressure by a phase shift approximately equal to $\pi/(2\gamma)$. According to Fig. 7, the induced pressure pulsation can be used as a measurable quantity in order to read, diagnose or for feedback to control the heating source.

5 Conclusions

Flow and heat transfer inside thin films supported by soft seals separating voids of stagnant fluid having a large value the volumetric thermal expansion coefficient have been analyzed in this work in the presence of suspended ultrafine particles in the coolant fluid. The thermal load was taken to be periodic. The governing continuity, momentum and energy equations were nondimensionalized and reduced to proper forms for small Reynolds numbers and negligible axial conduction. The deformation of the seal was related to the internal pressure and lower plate's temperature by theory of elasticity and a linearized model for thermal expansion. The velocity field and the solution of the energy equation were found using an iterative scheme and a marching technique in both the axial direction and time domains.

Increases in the coefficient of thermal expansion, dispersion parameter, fixation parameter and thermal squeezing parameter were found to cause enhancements in the cooling process. The thermal dispersion parameter was found to increase the stability of the thin film by decreasing fluctuation rates in the flow. The noise in the thermal load was found to affect the amplitude of the thin film thickness, Nusselt number and the lower plate temperature as well as their variations rate. However, it has a negligible effect on their mean values. Finally, flexible complex seals are useful in enhancing the cooling and can be used for additional purposes such as for diagnosing functions for heating sources as long as they possess large thermal expansion coefficient.

Acknowledgments

We acknowledge partial support of this work by DOD/DARPA/DMEA under grant number DMEA90-02-2-0216.

Nomenclature

A^* = a void dimension parameter
B = thin film length
C_F = volumetric thermal expansion correction factor
C^* = coefficient of thermal dispersion
c_p = average specific heat of the working fluid or the dilute mixture
D = width of the thin film
d_s = characteristic parameter of the seal
E = effective modulus of elasticity for the sealing assembly
G = width of the void
F_n = fixation parameter
F_T = dimensionless thermal expansion parameter
H, h, h_o = dimensionless, dimensional and reference thin film thicknesses
h_c = convective heat transfer coefficient
k = thermal conductivity of the working fluid or the dilute mixture
k_o = reference thermal conductivity of the fluid
Nu_L = lower plate's Nusselt number
P_S = thermal squeezing parameter
p = fluid pressure
q_o = reference heat flux at the lower plate
T, T_1 = temperature in fluid and the inlet temperature
t = Time
V_o = reference axial velocity
U, u = dimensionless and dimensional axial velocities
V, v = dimensionless and dimensional normal velocities
X, x = dimensionless and dimensional axial coordinates
Y, y = dimensionless and dimensional normal coordinates

Greek Symbols

β_q = dimensionless amplitude of the thermal load
β_T = coefficient of volumetric thermal expansion of the stagnant fluid
ε = perturbation parameter
γ = dimensionless frequency
μ = averaged dynamic viscosity of the working fluid or the dilute mixture
θ, θ_m = dimensionless temperature and dimensionless mean bulk temperature
θ_W = dimensionless temperature at the lower plate
ρ = averaged density of the working fluid or the dilute mixture
υ = averaged kinematic viscosity of the working fluid or the dilute mixture
τ, τ^* = dimensionless time
σ = squeezing number
ω = reciprocal of a reference time (reference squeezing frequency)
η = variable transformation for the dimensionless Y-coordinate
λ = dimensionless thermal dispersion parameter
Π = dimensionless pressure
Π_i = dimensionless inlet pressure
Λ = reference lateral to normal velocity ratio

References

[1] Moon, S. H., Yun, H. G., Hwang, G., and Choy, T. G., 2000, ''Investigation of Packaged Miniature Heat Pipe for Notebook PC Cooling,'' Int. J. Microcircuits Electron. Packag., **23**, pp. 488–493.

[2] Fedorov, A. G., and Viskanta, R., 2000, ''Three-Dimensional Conjugate Heat Transfer in the Microchannel Heat Sink for Electronic Packaging,'' Int. J. Heat Mass Transfer, **43**, pp. 399–415.

[3] Zhu, L., and Vafai, K., 1999, ''Analysis of a Two-Layered Micro Channel Heat Sink Concept in Electronic Cooling,'' Int. J. Heat Mass Transfer, **42**, pp. 2287–2297.

[4] Bowers, M. B., and Mudawar, I., 1994, ''Two-Phase Electronic Cooling Using Mini-Channel and Micro-Channel Heat Sink,'' ASME J. Electron. Packag., **116**, pp. 290–305.

[5] Hadim, A., 1994, ''Forced Convection in a Porous Channel With Localized Heat Sources,'' ASME J. Heat Transfer, **116**, pp. 465–472.

[6] Khaled, A.-R. A., and Vafai, K., 2002, ''Flow and Heat Transfer Inside Thin Films Supported by Soft Seals in the Presence of Internal and External Pressure Pulsations,'' Int. J. Heat Mass Transfer, **45**, pp. 5107–5115.

[7] Langlois, W. E., 1962, ''Isothermal Squeeze Films,'' Q. Appl. Math., **20**, pp. 131–150.

[8] Hamza, E. A., 1992, ''Unsteady Flow Between Two Disks With Heat Transfer in the Presence of a Magnetic Field,'' J. Phys. D, **25**, pp. 1425–1431.

[9] Bhattacharyya, S., Pal, A., and Nath, G., 1996, ''Unsteady Flow and Heat Transfer Between Rotating Coaxial Disks,'' Numer. Heat Transfer, Part A, **30**, pp. 519–532.

[10] Debbaut, B., 2001, ''Non-Isothermal and Viscoelastic Effects in the Squeeze Flow Between Infinite Plates,'' J. Non-Newtonian Fluid Mech., **98**, pp. 15–31.

[11] Khaled, A. R. A., and Vafai, K., 2003, ''Flow and Heat Transfer Inside Oscillatory Squeezed Thin Films Subject to a Varying Clearance,'' Int. J. Heat Mass Transfer, **46**, pp. 631–641.

[12] Li, Q., and Xuan, Y., 2002, ''Convective Heat Transfer and Flow Characteristics of Cu-Water Nanofluid,'' Sci. China, Ser. E: Technol. Sci., **45**, pp. 408–416.

[13] Xuan, Y., and Roetzel, W., 2000, ''Conceptions for Heat Transfer Correlation of Nanofluids,'' Int. J. Heat Mass Transfer, **43**, pp. 3701–3707.

[14] Friis, E. A., Lakes, R. S., and Park, J. B., 1988, ''Negative Poisson's Ratio Polymeric and Metallic Materials,'' J. Mater. Sci., **23**, pp. 4406–4414.

[15] Eastman, J. A., Choi, S. U. S., Li, S., Yu, W., and Thompson, L. J., 2001, ''Anomalously Increased Effective Thermal Conductivities of Ethylene Glycol-based Nanofluids Containing Copper Nanoparticles,'' Appl. Phys. Lett., **78**, pp. 718–720.

[16] Norton, R. L., 1998, *Machine Design; An Integrated Approach*, Prentice-Hall, New Jersey.

[17] Blottner, F. G., 1970, ''Finite-Difference Methods of Solution of the Boundary-Layer Equations,'' AIAA J., **8**, pp. 193–205.